Applied Physics B _####################_
https://doi.org/10.1007/s00340-019-7339-0

Applied Physics B
Lasers and Optics

Athermalization of a self-assembled rolled-up TiO_2 microtube ring resonator through incorporation of a positive thermo-optic coefficient material in planar bilayers

Abbas Madani[1,3] · Setareh Sedaghat[2]

Received: 25 January 2019 / Accepted: 29 October 2019

Abstract

For the first time, this paper theoretically and experimentally investigates the thermal stability of optical filters based on self-assembled TiO_2 rolled-up microtube ring resonators (RUMRs) by incorporating positive thermo-optic coefficient (TOC) materials (e.g., SiO_2 and/or Si_3N_4). The influence of the TOC, refractive index, and thickness of the positive TOC materials on the filtering performance of the TiO_2 RUMR is theoretically studied. The results illustrate that an increase in temperature leads to a blueshift in the resonant wavelength of the RUMR-based optical filter, which changes at a rate of -33.3 pm/K owing to the negative TOC of TiO_2 ($-4.9 \pm 0.5 \times 10^{-5}$/K). By increasing the thickness of SiO_2 or Si_3N_4 as a positive TOC material together with TiO_2, the temperature-induced resonant shifts of TiO_2/SiO_2 and/or TiO_2/Si_3N_4 RUMRs are theoretically obtained. The TIRS varies between -40 pm/K (-22 pm/K) and about 30 pm/K (22 pm/K) for TiO_2/SiO_2 (TiO_2/Si_3N_4) RUMRs. It is shown that thermal stability occurs when the thickness of the SiO_2 (Si_3N_4) layer is ~ 16 nm (12 nm). At the end of this study, as a proof of concept, an experiment is demonstrated by fabricating an RUMR based on TiO_2/SiO_2 on the flat silicon wafer. The experimental results show that the athermalization of the system is experimentally achieved by selecting the apricated thickness ratio of TiO_2/SiO_2. This novel approach for athermalization of the resonators opens up interesting perspectives on the implementation of vertical and multi-routing coupling between photonic and optoelectronic layers and more specifically in a three-integration fashion.

1 Introduction

Silicon photonics has been recognized as a mature and appealing platform for photonic integration, owing to its remarkable properties. This outstanding photonic platform can provide the opportunity to fulfill several functionalities on a single chip by following complementary metal oxide semiconductor (CMOS) fabrication technology [1, 2]. The high refractive index of silicon and the accessibility of high-quality oxides create possibilities for increasing the number of optical devices by fabricating a low-loss and ultracompact optical waveguide on a single chip [3–9]. Despite this great success in the field of silicon photonics, however, quantum photonics and quantum emitters are mainly operated in the visible wavelengths [10]. Hence, silicon photonic device suffers from non-transparency for visible wavelengths; hence, its application can be dramatically limited in this growing research field [10]. Apart from the materials perspective, silicon-based optical devices are highly wavelength dependent with temperature variations, due to their relatively high thermo-optical coefficient (TOC) (~ 1.84×10^{-4}/°C) [5–8]. This can be another important concern in integrated optics; by increasing the temperature in the device, an unwanted wavelength shift is caused in the system, which is not satisfactory for many important applications. For example, in the experiential demonstration of silicon photonics using multi-wavelength parallelism, optical filtering, switching and/or the implementation of dense 3D optoelectronic systems, this thermal heating may be one of the biggest obstacles in this system. Moreover, due to the fact that an electrically (optically) pumped semiconductor laser within the chip can

This article is part of topical collection on Optical Nanofibers and Microresonators (Síle Nic Chormaic, Misha Sumetsky, Lan Yang).

✉ Abbas Madani
a.madani@ifw-dresden.de; 812.abbas@gmail.com

[1] Institute for Integrative Nanosciences, IFW Dresden, Helmholtz str. 20, 01069 Dresden, Germany

[2] Department of Communications and Electronics, Shiraz University, Shiraz, Iran

[3] AMO GmbH, Aachen, Germany

Journal : Large 340 | Article No : 7339 | Pages : 11 | MS Code : 7339 | Dispatch : 7-11-2019

generate higher temperatures, an unwanted shift may occur in the laser beam, or some fluctuation and/or instability of the laser beam may occur. To end this unwanted issue, athermal operation of silicon photonic devices is crucial [11].

Hence, to stabilize the chip temperature to a constant level, the athermal photonic devices (Si or SiO_2 based) have been demonstrated extensively already [5–13]. One straightforward technique to fabricate athermal photonic devices (based Si or SiO_2) is to coat them with a polymer as the upper cladding layer and take advantage of the polymer's negative thermo-optic (TO) coefficient to neutralize the waveguide core's positive TOC coefficient. However, in the case of Si waveguides, because of the high thermo-optic coefficient of Si, the biggest challenge here is coupling almost half the light from the silicon core into the polymer cladding to satisfy the athermal condition. To solve this difficulty, in contrast to the other photonic materials (e.g., Si, InP, GaAs, SiO2), owing to its relatively strong negative TOC of approximately $\sim -1\times10^{-4}/°C$ and/or even $\sim -2\times10^{-4}/°C$ around 1550 nm (depending on the phase of TiO_2), it has recently presented itself as a valuable photonic material to stabilize chip temperature [13]. As a result, many groups have recently investigated the athermal operation of silicon photonic devices by over-cladding them, depositing TiO_2 on top of them. The CMOS-compatible fabrication has led to the hybrid system of TiO_2–Si devices (e.g., optical waveguides, ring resonators), which illustrates nearly complete cancelation of thermo-optical dependence in these hybrid devices. It is worth mentioning that a group at MIT has experimentally reported a blueshift (i.e., a shift to a shorter wavelength) in the resonant modes of microring resonators through an increase in temperature due to the relatively strong negative TOC of TiO_2 [12].

As a result, athermal microresonators have become attractive structures because of their insensitivity to temperature, strong confinement of light within a small volume and high Q factor for high-speed data transmission, as well as power reduction in optical communication systems and more importantly for thermal stability [3–8, 14–17]. Different types of athermal resonators such as microspheres, microdisks, microtoroids and microrings have been studied and fabricated already [18, 19]. One intriguing optical resonator [18] is based on a self-assembled rolled-up microtube (RUM) resonator. RUM resonators are easily integrated into coupled arrays, conveniently defined in materials design by thin film deposition techniques, and efficiently deployed with high sensitivity due to their hollow cores and ultrathin walls [20–28]. RUMs can be used for a broad range of photonic applications, including optofluidic components, optical signal processing and metamaterial devices [20, 22, 24, 25, 29, 30]. Like other photonic devices, the optical signals generated by RUMs are extremely vulnerable to changes in temperature, owing to their ultrathinness [24, 25].

In this paper, we propose for the first time the use of athermal rolled-up microtube (RUM) ring resonators to overcome temperature sensitivity. We suggest hybrid TiO_2–SiO_2 and/or TiO_2–Si_3N_4 RUMs as athermal resonators for optical filtering, which can greatly improve the thermal stability of TiO_2-based RUMs by incorporating SiO_2 and/or Si_3N_4, which possess a positive TOC and therefore the ability to compensate the commonly observed blueshift of TiO_2 RUM resonators.

To reach this goal, the general scheme of an athermal RUM resonator for optical filtering is outlined in Sect. 2. The theory of effective thermo-optic coefficients is presented in Sect. 3. In Sect. 4, the temperature sensitivity of TiO_2 RUMs for different temperatures and wall thicknesses is theoretically studied. Furthermore, the shift in optical resonances as a function of SiO_2 thicknesses and Si_3N_4 thicknesses with a fixed thickness of TiO_2 is investigated. In Sect. 4, the optical filtering performance of photonic RUMs, including wavelength shift and extinction ratio, is analyzed by a three-dimensional finite difference time domain (FDTD) method. Finally, as a proof of concept, an experiment is demonstrated by fabricating RUMs based on TiO_2–SiO_2 on the flat silicon wafer as substrate. To study the (in)sensitivity of the optical resonance modes to the temperature, the fabricated devices are excited under different input powers and the experimental results show that the non-shift of the optical modes is achieved, which may be a result of having an athermal hybrid RUM based on the appreciated thickness of these two materials. This novel idea is an important milestone in the implementation of vertical and multi-routing coupling between photonic layers in three optoelectronic devices, where the stability of the optical signals is really essential.

2 Scheme of the on-chip hybrid (athermal) rolled-up microtube ring resonator

A 3D layout of an optical filter based on an athermal hybrid RUM resonator is proposed in Fig. 1a, which is monolithically integrated with a nanophotonic waveguide. This suggested device is composed of a hybrid RUM, which is coupled to a straight single-mode silicon waveguide located on the substrate surface. Similar to our previous works [25, 31], the proposed device can be easily fabricated on a silicon wafer coated with SiO_2. By following the parameters from our previous works, in this theoretical work, on-chip silicon waveguides are set to a 220-nm-thick silicon layer on 4-μm-thick SiO_2 to avoid any coupling light to the substrate. To experimentally study the temperature dependence of our novel hybrid resonator, it is feasible to implement the electrodes next to the waveguides and integrate them with the RUM (see outlook for more details and/or [28]). In this scheme, the electrode can be designed on top of the 2D nanomembrane, and when the nanomembrane is

Journal : Large 340 | Article No : 7339 | Pages : 11 | MS Code : 7339 | Dispatch : 7-11-2019

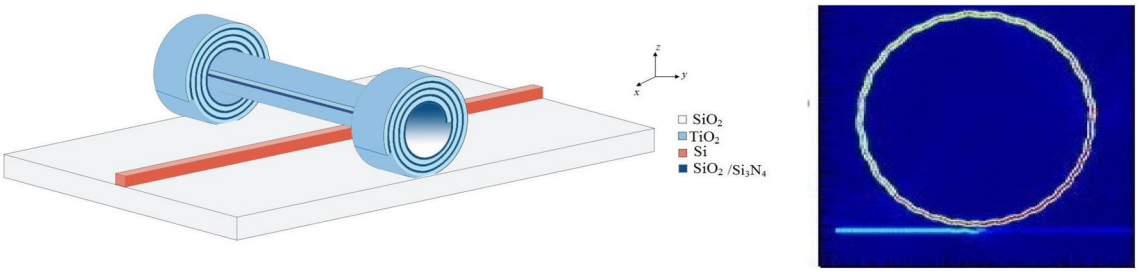

Fig. 1 Schematic of the proposed athermal optical filter based on an RUM, composed of a TiO_2/SiO_2 (TiO_2/Si_3N_4) bilayer, positioned on top of a straight silicon waveguide on an SiO_2 substrate

rolled up, the electrodes are monolithically integrated within the tube windings [29, 32]. However, in our theoretical investigation, we simply change the temperature in the software used, which leads to changes in the refractive index that are then automatically considered in our calculation. We simply used the FDTD solution of LUMERICAL software. In this software, there is a model for each material that the TOC can introduce. Moreover, there is the possibility of adjusting the operating temperature to the desired value for this quantity.

For example, if the device must be simulated at a temperature of 312 K, the operating temperature is set to 312, whereas the TOC of the material is constant. In the system under study, the silicon waveguide with a cross section of 400×210 nm^2 was chosen to realize single-mode transmission. Furthermore, 16-μm TiO_2–SiO_2 (TiO_2–Si_3N_4) RUM in the free-standing part was utilized. The parameters were tailored such that the effective index of the RUM (n_{eff}=2.076 at $\lambda=1.55$ μm) matched the effective index of the single-mode silicon waveguide. The optical profile of this proposed athermal TiO_2 RUM-based filter is depicted in Fig. 1b, where the temperature is set to room temperature (300 K) and the resonant wavelength is 1546.84 nm. A 60-nm gap between athermal RUM and silicon waveguide is engineered for a maximum transmission coefficient [26, 27].

3 Theory of effective thermo-optic coefficient (TOC)

It is known that thermal heating induces a temperature-dependent refractive index change in the constituent materials. For the RUM resonator, changing the temperature leads to a change in the index of the resonator material and consequently leads to a shift in the resonant wavelength λ_0 toward a shorter (blueshift) or longer (redshift) wavelength. The shift with respect to temperature, which is called a temperature-induced resonant shift (TIRS), is given by [9]:

$$\frac{d\lambda}{dT} = \frac{\partial n_{eff}}{\partial T}\frac{\lambda_0}{n_g}, \tag{1}$$

where λ_0 is the resonant wavelength, n_{eff} is the effective index, T is the temperature, and n_g is the group index. In Eq. 1, we assume that the optical mode is tightly confined within the tube wall. Therefore, n_{eff} corresponds to the effective refractive index of RUM by considering power confinement within individual regions such as the tube wall, hollow core, and surrounding region. Owing to the asymmetric AQ6 geometry of RUM (see Fig. 1a), the analytically calculated values need to be considered for three parts of the RUM (i.e., the two leg parts and a middle part). By taking advantage of the coupling area between RUM and optical waveguide, only the middle part of RUM needs to be considered, which was already analytically calculated in our previously published works [9, 12]. It should be noted that the terms in Eq. 1 are wavelength dependent. To decrease or eliminate the temperature dependence of the RUM, it is suggested to use materials with the opposite thermo-optic coefficient in planar grown bilayers, which can be a promising scheme to achieve athermalization. In this regard, the effective index of the whole RUM structure will change in Eq. 1. Therefore, the effective thermo-optic coefficient of the RUM wall before rolling up is

$$n_{eff} = \Gamma_o n_o + \Gamma_a n_a, \tag{2}$$

where Γ_o and Γ_a are modal confinement factors for original and athermal layers, and n_o and n_a are refractive indices of these regions, respectively. Consequently, the effective thermo-optic coefficient becomes

$$\frac{\partial n_{eff}}{\partial T} = \Gamma_o \frac{\partial n_o}{\partial T} = \Gamma_a \frac{\partial n_a}{\partial T}. \tag{3}$$

In this work, the modal confinement and positive TOC of the athermal layer (SiO_2, Si_3N_4) are engineered to balance the modal confinement and negative thermo-optic coefficients of the RUM wall (TiO_2).

3.1 Filtering performance, thermal stability, and athermalization

To filter the specific wavelength using conventional (and/or athermal) RUM, a winding number and asymmetric parameter should be engineered. For optical filtering, standard wavelength in telecom band (O-band to C-band), asymmetric parameter, and wall thickness of TiO_2 RUM are considered $5\pi/4$ and 345 nm, respectively. Furthermore, it has already been found that the TOCs of TiO_2, SiO_2, and Si_3N_4 are -4.5×10^{-5}/K [12], $+2\times10^{-5}$/K [11], and $+4\times10^{-5}$/K [9], respectively. All simulations are based on the 66th azimuthal mode and the first radial mode.

When the device serves as an optical filter, a broadband light (including $\lambda_1 \ldots \lambda_i \ldots \lambda_n$ wavelengths) from the input port coupled to the RUM, then the specific wavelength (i.e., λ_i)—which is called resonance mode—separates from the input signal according to the resonance condition and also the properties of the RUM along the axial direction, and finally sends the rest of the input wavelengths ($\lambda_1 \ldots \lambda_{i-1}, \lambda_{i+1} \ldots \lambda_n$) to the through port. Figure 2a shows the influence of temperature on the transmission spectrum of an optical filter based on 16 μm TiO_2 RUM with three winding numbers (for more information about our simulation technique, see [26–28]). As illustrated in Fig. 2a, the wavelength 1546.84 nm is filtered at 300 K (room temperature), and by increasing the temperature to 312 K, the filtered wavelength experiences blueshift (i.e., shift to the shorter wavelength) because of the negative TOC of TiO_2. Hence, the effect of temperature on the resonant wavelength for an RUM based on TiO_2 with a diameter of 16 μm at the different winding numbers is presented in Fig. 2b. This figure indicates that when the temperature increases, the resonance modes are clearly shifted to the shorter wavelength.

As can be easily calculated, the resonance peaks as a function of temperature yields a rate of $d\lambda_0/dT = -33.3$ pm/K for the different winding numbers, which corresponds to a $dn/dT = 5.8\times10^{-5}\ k^{-1}$. As mentioned above, this blueshift in the resonant wavelength results from the negative TOC of TiO_2. Moreover, a variation in the resonant wavelengths as a function of winding numbers is shown in Fig. 2b. This phenomenon leads to the much larger effective refractive index, which will result in higher mode confinement. Since the resonant wavelength varies directly in relation to the effective refractive index, it can be observed that the resonant wavelength increases as the wall thickness increases. In Fig. 3, resonant modes characteristic of the athermal TiO_2 microtube are represented by overlaying an SiO_2 layer on TiO_2 bilayer membrane at different temperatures (which vary between 304 and 312 K). As a result, by increasing the thickness of the SiO_2 layer a redshift in the resonant wavelengths occurs due to the positive TOC of SiO_2 ($+2\times10^{-5}$/K), as well as increasing the whole thickness of the tube wall.

It is also worth mentioning that the effective refractive index in TiO_2/SiO_2 RUM is not the same as pure TiO_2 RUM, because of the dissimilar refractive indices of pure TiO_2 ($n_{TiO_2} = 2.45$) and SiO_2 ($n_{SiO_2} = 1.44$). As a result, it can be explained why the resonant wavelengths are different in these two types of RUMs (pure TiO_2 RUM and hybrid TiO_2 RUM) such that the TiO_2–SiO_2 RUM with a thicker wall presents a shorter resonant wavelength shift than RUM composed only of TiO_2 with 345-nm thickness (because the effective refractive index of hybrid RUM is much smaller than that of pure TiO_2 RUM). Therefore,

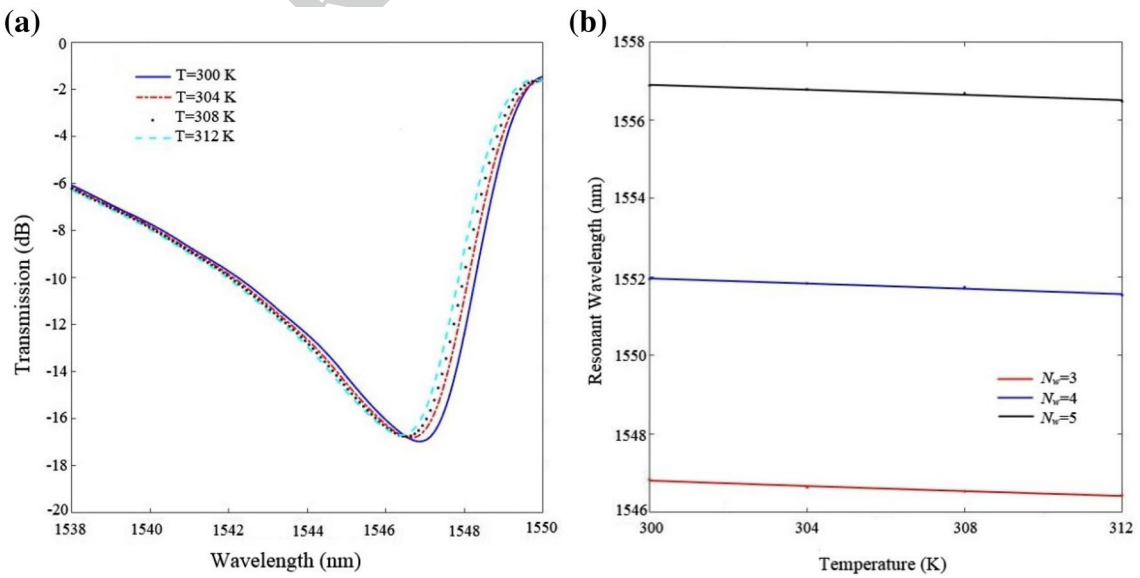

Fig. 2 **a** Transmission spectrum of an 8-μm-radius TiO_2 with wall thickness of 345 nm at different temperatures

Journal : Large 340 | Article No : 7339 | Pages : 11 | MS Code : 7339 | Dispatch : 7-11-2019

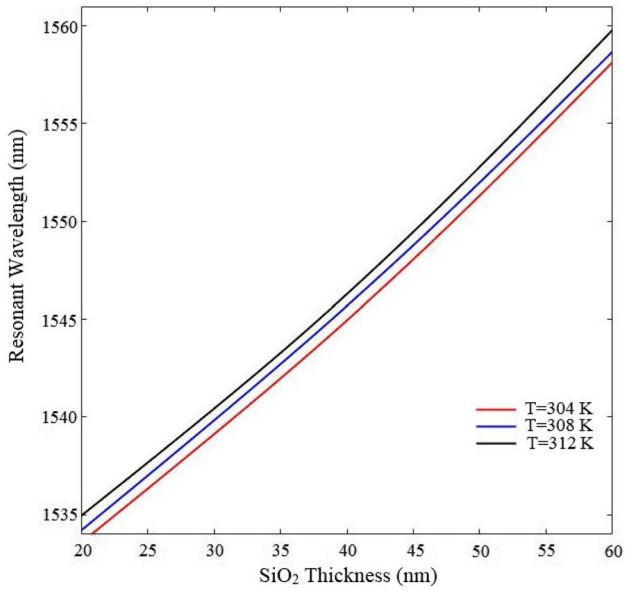

Fig. 3 Variations of the resonant wavelength of TiO_2–SiO_2 microtube versus the thickness of SiO_2 layer with a constant TiO_2 thickness of 115 nm

Table 1 Shift in resonant wavelength of TiO_2 microtube by utilizing different thicknesses of the SiO_2 layer between 40 and 45 nm at 304 K

SiO_2 thickness (nm)	Resonant wavelength (nm)
41	1545.74
42	1545.54
43	1546.05
44	1546.84
45	1547.74

Table 2 Shift in resonant wavelength of TiO_2 microtube by utilizing different thicknesses of the SiO_2 layer between 40 and 45 nm at 308 K

SiO_2 thickness (nm)	Resonant wavelength (nm)
41	1545.52
42	1546.04
43	1546.84
44	1547.44
45	1548.2

the range of thickness of SiO_2 layers for athermalization must be increased from 40 to 45 nm, as shown in Fig. 3. Further simulation results are presented in Tables 1, 2, and 3 (see "Appendix"). It is indicated that to generate an athermalization behavior in our hybrid RUM, the appreciated thickness of SiO_2 needs to be 44 nm at 304 K, 43 nm at 308 K, and 41 nm at 312 K.

Table 3 Shift in resonant wavelength of TiO_2 microtube by utilizing different thicknesses of the SiO_2 layer between 40 and 45 nm at 312 K

SiO_2 thickness (nm)	Resonant wavelength (nm)
41	1546.85
42	1547.54
43	1548.34
44	1549.04
45	1549.95

A trend in the temperature-induced resonant shift (TIRS) in the athermal TiO_2/SiO_2 RUM versus the thickness of the SiO_2 layer is plotted in Fig. 4a, wherein the total thickness of bilayers remains constant at 115 nm. As can be seen in this figure, by increasing the thickness of SiO_2 from 5 up to 30 nm, the resonant wavelength shifted toward the longer wavelengths. As the results from TIRS AQ8 show, it can be increased from a range of − 40 pm/K to about 30 pm/K. This figure proposes that by choosing the thickness of SiO_2 around 16 nm, TIRS compensation can be well achieved.

Furthermore, athermalization of TiO_2 RUM utilizing Si_3N_4, whose refractive index ($n_{Si_3N_4} = 1.99$) is much closer to the refractive index of TiO_2 (at the telecom wavelength), is shown in Fig. 4b. In this figure, the total thickness of bilayers is still 115 nm. Figure 4b shows the TIRS under the influence of changing the thickness of Si_3N_4 for the hybrid TiO_2–Si_3N_4 RUM.

As expected, TIRS compensation occurs with a smaller thickness of Si_3N_4 ($t_{Si_3N_4} = 12$ nm) as compared with SiO_2, owing to the closer refractive index of Si_3N_4 with respect to TiO_2. Additionally, more light confinement between these layers is elegantly expected. By comparing the athermalizing behavior of these two hybrid RUMs (i.e., TiO_2–SiO_2 and TiO_2–Si_3N_4 RUMs), it is found that the smoother variations of TIRS with respect to the thickness of the athermal layer can be achieved by selecting the material which has a closer refractive index to the original planar bilayers of an RUM. As a conclusion and prior to the experimental part, the TOC of both materials has already been known (i.e., TiO_2 and SiO_2), and by following $\frac{dn_{eff}}{dT}$ (and/or $\frac{d\lambda_0}{dT}$) and wavelength shift ($\Delta\lambda$), it is feasible to estimate the value for the temperature. Based AQ9 on the calculations, when the input power was 85μW, the temperature within the RUM will be estimated to be 25 °C and at 1.7 mW changed to around 65 °C.

Journal : Large 340 | Article No : 7339 | Pages : 11 | MS Code : 7339 | Dispatch : 7-11-2019

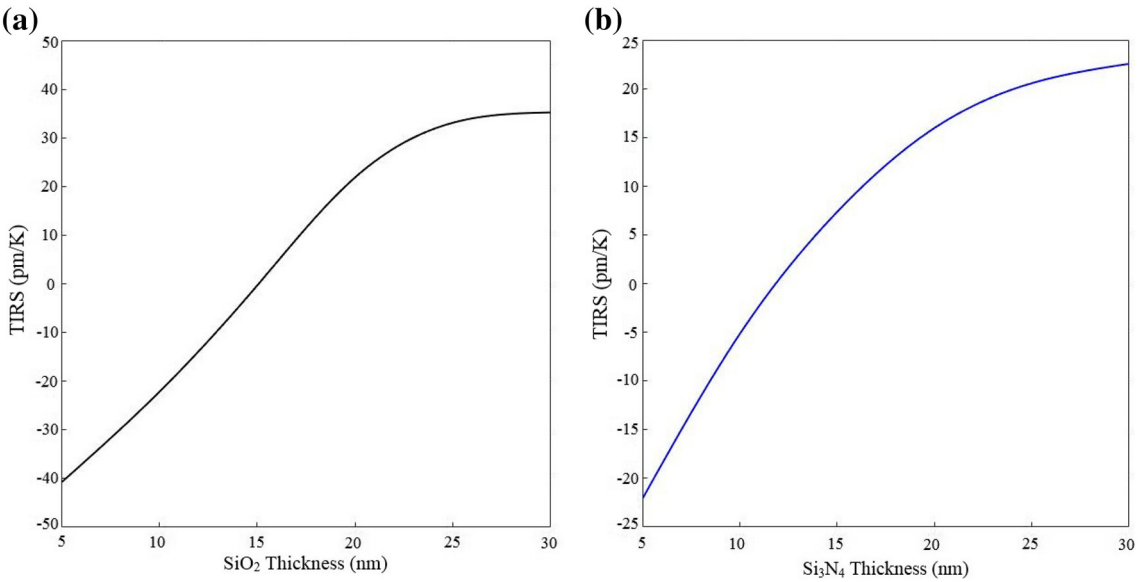

Fig. 4 **a** Temperature-induced resonant shift (TIRS) of TiO_2–SiO_2 RUM as a function of the thickness of SiO_2 layer, while the total thickness of the RUM remains constant at 115 nm

4 Experimental part

4.1 Fabrication of the hybrid (athermal) RUMs based on TiO_2–SiO_2

A theoretical study of athermal resonators-based on-chip hybrid RUMs was conducted, followed by an investigation into how the thickness variation of SiO_2 and/or Si_3N_4 within the TiO_2 RUMs' walls can influence the performance of these proposed devices. In this section, as a proof of concept, the fabrication of the isolated (i.e., not integrated with photonic waveguides) athermal TiO_2 RUMs in combination with SiO_2 is presented. To study the temperature-(in)sensitive resonance modes, the fabricated devices are excited using a continuous wavelength (CW) laser ($\lambda = 442$ nm) under different exciton powers.

The devices are fabricated using an elegant well-established roll-up method which has been discussed extensively in the literature [20–25, 29–31, 33–36]. A schematic of the fabrication procedure is shown in Fig. 5. Standard photolithography was used to fabricate an array of U-shaped [25, 31, 33, 35] photoresist (AR-P 3510, Allresist GmbH) patterns on an Si substrate [25, 35]. The photoresist pattern

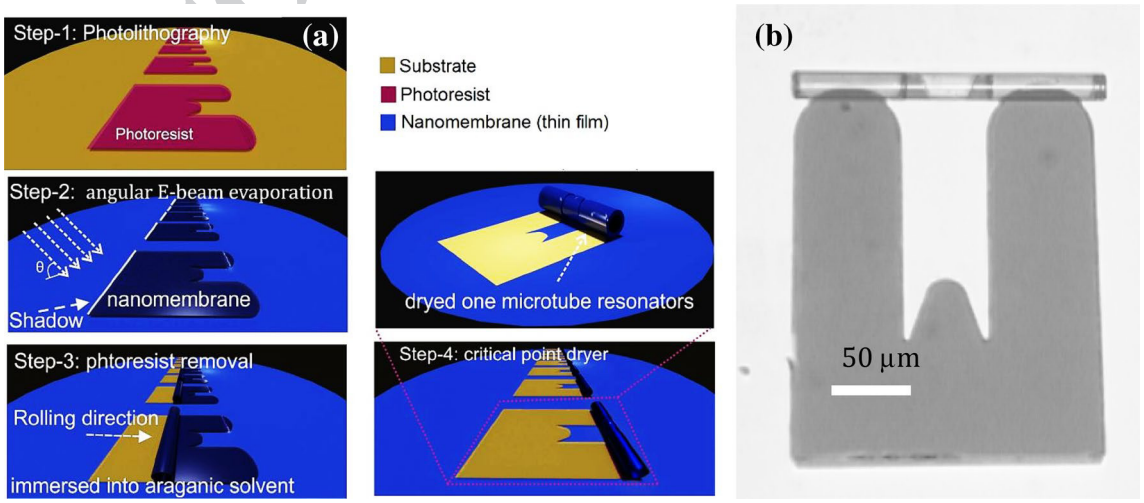

Fig. 5 **a** Schematic of the fabrication procedure of microtubes from a photoresist sacrificial layer

Journal : Large 340 | Article No : 7339 | Pages : 11 | MS Code : 7339 | Dispatch : 7-11-2019

(with a thickness of around 2 μm) defines the final shape of the RUM and serves as a sacrificial layer.

Then, a 115-nm-thick layer of differentially strained TiO_2–SiO_2 is deposited on the surface using tilted electron beam evaporation [20, 25, 31, 33]. It is worth mentioning that in this fabrication process, TiO_2 was deposited from pure titanium pellets (Kurt J. Lesker Company) in an oxygen background (the pressure inside the chamber was 2.6×10^{-4} mbar), with strain being generated by depositing parts of the layer at different rates. To fabricate the first sample (called "device no. 1" in this paper), the SiO_2 layer was deposited with a low (about ≈ 0.3 Å/s) deposition rate and a thickness of 15 nm, and then the TiO_2 layer (with a thickness of 100 nm) as second layer was deposited with a high (about ≈ 3.4 Å/s) deposition rate. For fabricating the second sample (called "device no. 2" in this paper), the SiO_2 layer was deposited with a low (about ≈ 0.4 Å/s) deposition rate and a thickness of 25 nm, and then the TiO_2 layer (with a thickness of 90 nm) as a second layer was deposited with a high (about ≈ 3.8 Å/s) deposition rate. The photoresist was then dissolved with dimethyl sulfoxide (DMSO; VWR International S.A.S.), leading to relaxation of the nanomembrane, which is rolled up into RUMs with an average diameter of 10 μm, and then dried in a critical point dryer to avoid collapse due to surface tension. It is worth mentioning that after rolling, the tube sits on the vertical wall formed by the material deposited on the side of the sacrificial layer. This feature is important to avoid light losses to the substrate when the microtube is employed as an optical microcavity. As an example, Figs. 5b and 6b show the top of the viewed optical images of the RUMs (with different lobs) fabricated in this manner. In both figures, the outline of the U-shaped pattern is clearly visible. In the inset of Fig. 6b, details of the RUMs are shown which highlight the high quality of the fabrication process. The membrane is rolled tightly—so that the windings are in contact with each other—and completely. The bridge-like middle segment is elevated above the substrate to prevent optical leakage, and the axial mode-inducing lobe-like patterns on the middle segment and both ends are clearly defined.

4.2 Optical characterization and results

In this work, the optical characterization (i.e., excitation and detection of optical resonant modes) from the fabricated athermal microtubes (with different thicknesses of SiO_2) is performed using a commercial confocal laser μ-PL spectroscopy at room temperature, supplied by Renishaw inVia, as schematically depicted in Fig. 6a. It should be remarked that a μ-PL experiment is a free-space approach for excitation of the resonance modes within the RUMs. It has been reported in [20, 31, 37] that the origin of PL emission in these fabricated devices is likely silicon nanocrystals embedded in SiO_2 for light, and also trace amounts of residual photoresist on the sample and/or unspecified defect centers similar to those found in silica.

However, it is proof that the titanium dioxide material of the tube wall has very poor PL properties [31]. However, this drawback of using TiO_2 microtubes can be easily addressed by using SiO_2 as another layer of the tube's material. A μ-PL AQ17 setup was performed using an He–Cd laser with an excitation line of 442 nm. The pump beam is routed and focused through a 50× microscopic objective lens (with a spot size of ≈ 1 μm^2) onto the fabricated RUMs, which is mounted to a precision XYZ stage. The luminescence signals from the examined tube are collected by the same objective and diffracted in an optical spectrometer with 1200 lines/mm. An electrically cooled charge-coupled device (CCD) camera was used for spectral analysis.

After exciting the athermal RUM (device no. 1 or device no. 2) using the incident laser beam, the silicon nanocrystals embedded in the SiO_2 within the tube wall emit light which can propagate and circulate in the ring-like microtube nanomembrane wall. When the wavelength of the emitted light satisfies the constructive interference condition $\pi D = m\lambda/n$ (where D is the tube diameter, m is the integer

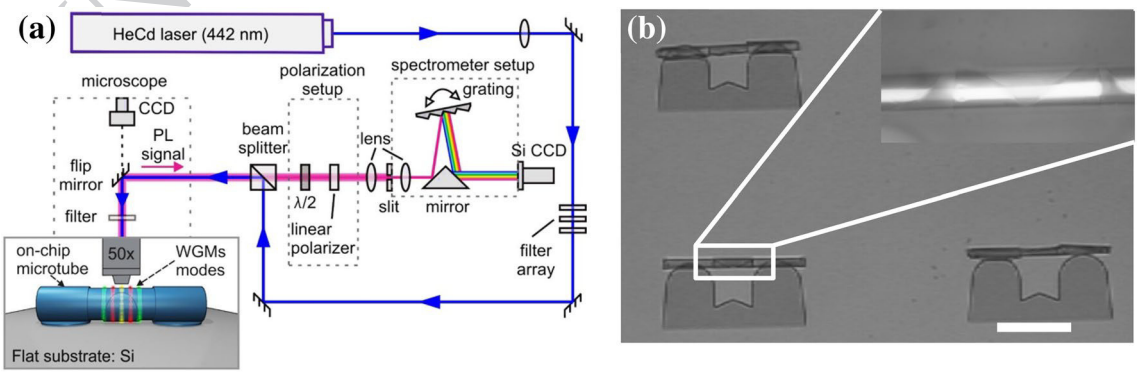

Fig. 6 **a** Schematic illustration of the micro-PL setup to excite and detect optical resonances

Journal : Large 340 | Article No : 7339 | Pages : 11 | MS Code : 7339 | Dispatch : 7-11-2019

mode number, λ is the resonant wavelength, and n is the refractive index of the tube wall), optical resonance modes are formed as the peaks on top of the PL background in a fixed spectral range from 550 to 850 nm. To show the results more clearly, only small parts of this large spectral range are shown in Figs. 7b and 8b as different colors under different excitation powers, respectively.

The set of the peaks shown have FSRs = 10 nm and 8 nm, respectively, which is the difference between two adjacent fundamental peaks that is in good agreement with the calculated value (by the simple equation $\mathrm{FSR} = \frac{\lambda_{\mathrm{res}}^2}{n\pi D}$, where n is the refractive index, D is the diameter of RUM, and λ_{res} is the wavelength of the resonant mode). Apart from the observation of resonance modes from the athermal RUMs (device no. 1), as shown in Fig. 8b, the device (with a thickness of 15 nm of SiO_2 within the tube's wall) was excited with different powers using a μ-PL setup. Figure 7b displays the results of a less than 2 nm shift in the optical modes at different powers (blueshift or shot to the shorter wavelength).

Because of the negative TOC of the TiO_2, this blueshift can occur. Based on our theoretical work, we find that it is necessary to increase the thickness of SiO_2 to overcome this blueshift. By following the apricated thickness of the TiO_2 and SiO_2 (i.e., SiO_2 layer with a thickness of 25 nm and then the TiO_2 layer with a thickness of 90 nm, respectively), now the fabricated device acts as the athermal microtube. Optical characterization of the fabricated device no. 2 shows non-shift of resonance modes, while the exaction power of the laser increases (or in other words, while the temperature of the tube increases).These non-shifted modes can be explained by the fact that the negative TOC of TiO_2 causes a shift to the shorter wavelengths (a blueshift) around 2 nm, while the positive TOC of SiO_2 with the apricated thickness (i.e., $t_{SiO2} = 25$ nm) leads to an equal shift ($\Delta\lambda = 2$ nm) but toward the longer wavelengths (a redshift). Thus, in the

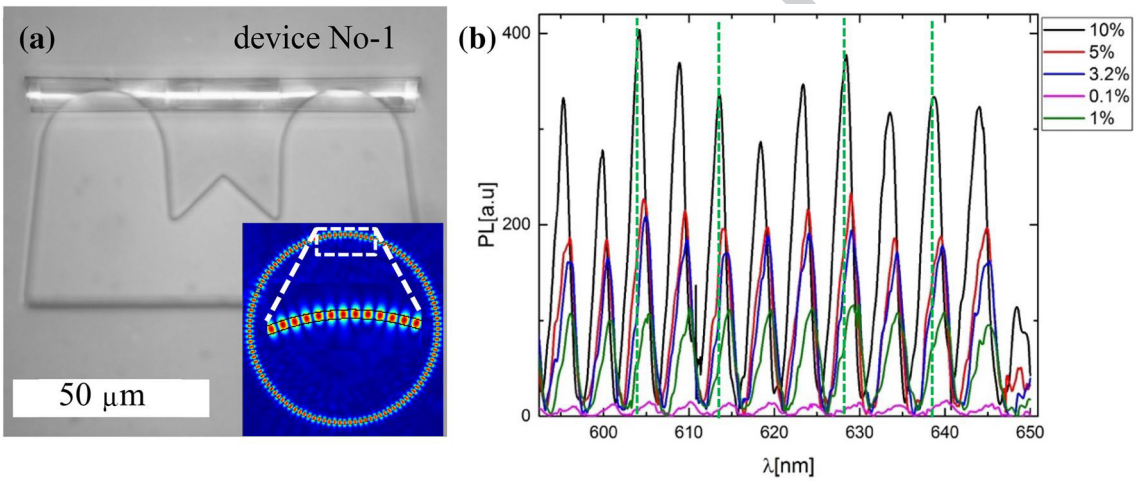

Fig. 7 **a** Top view optical microscopy image of a hybrid RUM (with a thickness of 15 nm of SiO_2 and 100 nm of TiO_2 layer)

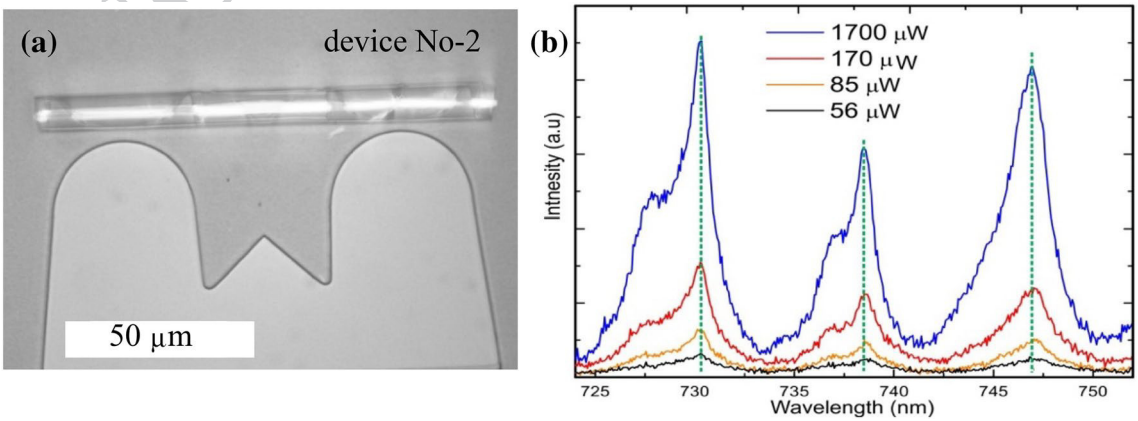

Fig. 8 **a** Top view optical microscopy image of an athermal RUM (with a thickness of 25 nm of SiO_2 and 90 nm of TiO_2 layer)

Journal : Large 340 | Article No : 7339 | Pages : 11 | MS Code : 7339 | Dispatch : 7-11-2019

experiment, it is proven that the unwanted shift can easily disappear when the apricated thickness ratio between two materials is selected, as shown in Fig. 9b. Additional optical measurements are performed for other athermal devices, exhibiting similar results to those presented in Fig. 9b. This validates the feasibility of athermal mass production of RUMs. In our work, we used TiO_2–SiO_2 as an example material, but the fabrication process can be easily adapted to RUMs made out of other materials such as TiO_2–Si, TiO_2–SiOX, TiO_2–SiN_x, or TiO_2–$Y2O_3$.

4.3 Future outlook

In this paper, monolithic integration of athermal RUMs on photonic waveguides is proposed and theoretically investigated. Apart from this idea, it would be of great interest to experimentally demonstrate and fabricate this device, which would be a crucial ingredient for advanced optoelectronic applications such as 3D stacked chip integration.

Figure 9 represents an artistic view of an on-chip athermal rolled-up microtube which is monolithically integrated with optical waveguides, as an example. As shown in Fig. 9a, the 2D nanomembrane can be designed well on top of the electrode, and it is rolled up together with the electrodes to form a tubular shape [37]. In this way, the electrodes are monolithically integrated with tube windings (see Fig. 9b). It is worth stating that in recent years, a step forward in integrating the rolled-up microtube onto planar waveguides or other photonic as well as integration electrodes within tube winding has been realized by our group and other research groups (see Fig. 10 as an example).

To achieve a fully integrated system with a low cost and ultracompactness, and to use it in different areas, more attention should be paid to this proposal for bringing these two possibilities (i.e., integrating waveguides and electrodes into one single tube) within a single athermal RUM, as the next step.

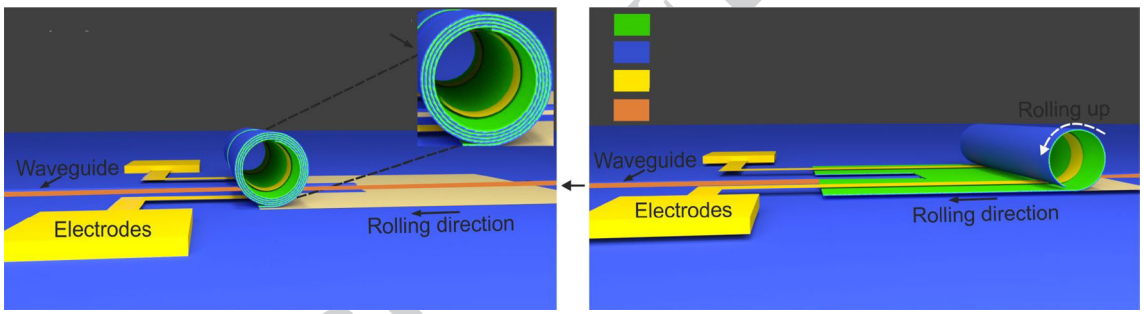

Fig. 9 **a** and **b** Schematic of the proposed athermal optical filter based on an RUM, composed of a TiO_2/SiO_2 (TiO_2/Si_3N_4) bilayer, positioned on top of a straight silicon waveguide and electrodes on an SiO_2 substrate

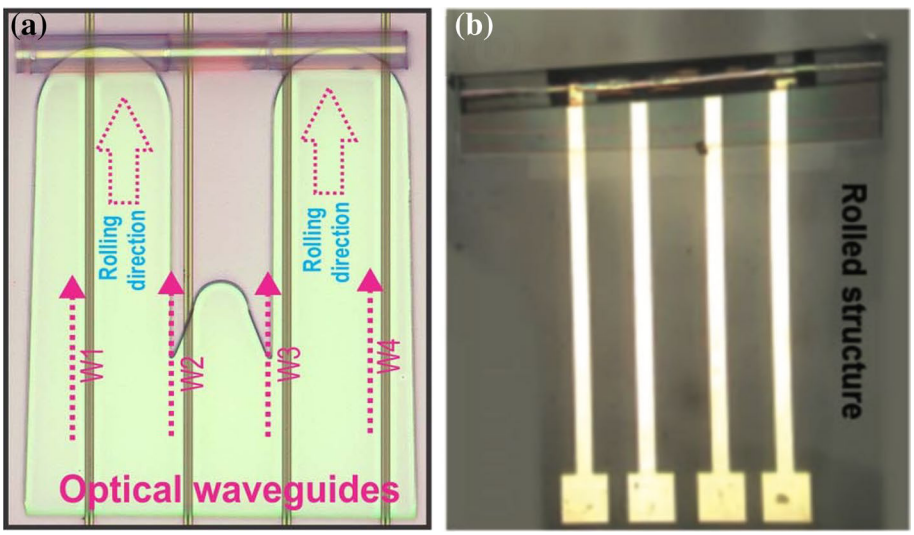

Fig. 10 **a** Top view optical microscopy image of a TiO_2 RUM fully integrated with nano-waveguides on a single chip. Taken with permission from Ref [25]

Journal : Large 340 | Article No : 7339 | Pages : 11 | MS Code : 7339 | Dispatch : 7-11-2019

5 Conclusion

One important concern in integrated optics is thermal heating, which leads to unwanted wavelength shifts in the integrated system. This shift is often unsuitable for important applications: for example, optical filtering. To this end, it is necessary to fabricate athermal resonators instead of the conventional resonators in the integrated system. In this study, an athermal TiO_2 RUM with SiO_2 (Si_3N_4) layer is proposed and designed for filtering with thermal stability. The transmission spectra and filtering performance of TiO_2 RUM are investigated at different temperatures. The simulation results indicate that the negative TOC of TiO_2 leads to a blueshift in resonant wavelength with different wall thicknesses; consequently, the rate of wavelength shift is − 33.3 pm/K. To compensate for the shift in wavelength, the behavior of TIRS in an athermal TiO_2/SiO_2 (TiO_2/Si_3N_4) RUM versus an SiO_2 (Si_3N_4) layer thickness—where SiO_2 and Si_3N_4 are positive TOC materials—is studied. The results show that increasing SiO_2 (Si_3N_4) thickness results in redshift of the resonant wavelengths, and this increment leads to increasing TIRS in the ranges of − 40 pm/K and about 30 pm/K, and − 22 pm/K and 22 pm/K, for TiO_2/SiO_2 and TiO_2/Si_3N_4 RUMs, respectively. Also, compensation is achieved at a thickness of ~ 16 nm and 12 nm for the SiO_2 and Si_3N_4 layers respectively.

Finally, for a proof of concept, an experiment is made on fabricating RUMs based on TiO2/SiOx on the flat silicon wafer as substrate. They were excited with different powers using a μPL setup. The result confirms the athermal idea by displaying the non-shift of the optical modes at different powers.

Appendix

In this section, athermalization of TiO_2/SiO_2 RuM by modifying SiO_2 thickness when the thickness of TiO_2 layer is 115 nm is investigated in Tables 1, 2, and 3 for operating temperatures 304 K, 308 K, and 312 K, respectively.

References

1. D.A.B. Miller, Optical interconnects to electronic chips. Appl. Opt. **49**, F59–F70 (2010)
2. M. Smit, J. van der Tol, M. Hill, Moore's law in photonics. Laser Photonics Rev. **6**, 1–13 (2012)
3. J.D. Suter, I.M. White, H. Zhu, X. Fan, Thermal characterization of liquid core optical ring resonator sensors. Appl. Opt. **46**, 389 (2007)
4. M.R. Foreman, W.-L. Jin, F. Vollmer, Optimizing detection limits in whispering gallery mode biosensing. Opt. Express **22**, 5491 (2014)
5. J. Teng, P. Dumon, W. Bogaerts, H. Zhang, X. Jian, X. Han, M. Zhao, G. Morthier, R. Baets, Athermal Silicon-on-insulator ring resonators by overlaying a polymer cladding on narrowed waveguides. Opt. Express **17**, 14627 (2009)
6. V. Raghunathan, W.N. Ye, J. Hu, T. Izuhara, J. Michel, L.C. Kmerling, Athermal operation of Silicon waveguides: spectral, second order and footprint dependencies. Opt. Express **18**, 17631 (2010)
7. S. Feng, K. Shang, J.T. Bovington, R. Wu, B. Guan, K.T. Cheng, J.E. Bowers, S.J.B. Yoo, Athermal silicon ring resonators clad with titanium dioxide for 1.3 μm wavelength operation. Opt. Express **23**(20), 25653–25660 (2015)
8. V. Raghunathan, T. Izuhara, J. Michel, L. Kimerling, Stability of polymer-dielectric bi-layers for athermal silicon photonics. Opt. Express **20**(14), 16059–16066 (2012)
9. S. Namnabat, K. Kim, A. Jones, R. Himmelhuber, C. DeRose, D. Trotter, A. Starbuck, A. Pomerene, A. Lentine, R. Norwood, Athermal silicon optical add-drop multiplexers based on thermo-optic coefficient tuning of sol-gel material. Opt. Express **25**, 21471–21482 (2017)
10. J.T. Choy, J.D.B. Bradley, P.B. Deotare, I.B. Burgess, ChC Evans, E. Mazur, M. Lončar, Integrated TiO_2 resonators for visible photonics. Opt. Lett. **37**, 539–541 (2012)
11. F. Qiu, A.M. Spring, S. Yokoyama, Athermal and high-Q hybrid TiO_2–Si_3N_4 ring resonator via an etching-free fabrication technique. ACS Photonics **2**, 405–409 (2015)
12. O. Reshef, K. Shtyrkova, M.G. Moebius, S. Griesse-Nascimento, S. Spector, C.C. Evans et al., Polycrystalline anatase titanium dioxide microring resonators with negative thermo-optic coefficient. J. Opt. Soc. Am. B **32**, 2288–2293 (2015)
13. F. Ou, X. Li, B. Liu, Y. Huang, S.-T. Ho, Enhanced radiation-loss-based radial-waveguide-coupled electrically pumped microresonator lasers with single-directional output. Opt. Lett. **35**, 1722–1724 (2010)
14. I. Teraoka, Analysis of thermal stabilization of whispering gallery mode resonance. Opt. Commun. **310**, 212 (2014)
15. S. Lane, Y. Zhi, F. Marsiglio, A. Meldrum, Refractometric sensitivity and thermal stabilization of fluorescent core microcapillary sensors: theory and experiment. Appl. Opt. **6**, 1331–1340 (2015)
16. F. Qiu, F. Yu, A.M. Spring, Sh Yokoyama, Athermal silicon nitride ring resonator by photobleaching of Disperse Red 1-doped poly (methyl methacrylate) polymer. Opt. Lett. **37**, 0146–9592 (2012)
17. F. Qiu, F. Yu, A.M. Spring, Sh Yokoyama, Complementary metal–oxide–semiconductor compatible athermal silicon nitride/titanium dioxide hybrid micro-ring resonators. Appl. Phys. Lett. **102**, 051106 (2013)
18. K.J. Vahala, Optical microcavities. Nature **424**, 839–846 (2003)
19. M.S. Luchansky, R.C. Bailey, High-Q optical sensors for chemical and biological analysis. Anal. Chem. **84**, 793–821 (2012)
20. S.M. Harazim, W. Xi, C.K. Schmidt, S. Sanchez, O.G. Schmidt, Fabrication and applications of large arrays of multifunctional rolled-up SiO/SiO_2 microtubes. J. Mater. Chem. **22**, 2878–2884 (2012)
21. J. Zhang, J. Zhong, Y.F. Fang, J. Wang, G.S. Huang, X.G. Cui et al., Roll up polymer/oxide/polymer nanomembranes as a hybrid optical microcavity for humidity sensing. Nanoscale **6**, 13646–13650 (2014)
22. G. Huang, V.A. Bolaños Quiñones, F. Ding, S. Kiravittaya, Y. Mei, O.G. Schmidt, Rolled-up optical microcavities with subwavelength wall thicknesses for enhanced liquid sensing applications. ACS Nano **4**, 3123–3130 (2010)
23. S.M. Harazim, V.A. Bolanos Quinones, S. Kiravittaya, S. Sanchez, O.G. Schmidt, Lab-in-a-tube: on-chip integration of glass optofluidic ring resonators for label-free sensing applications. Lab Chip **12**, 2649–2655 (2012)

Journal : Large 340 | Article No : 7339 | Pages : 11 | MS Code : 7339 | Dispatch : 7-11-2019

24. A. Madani, S.M. Harazim, V.A. Bolaños Quiñones, M. Kleinert, A. Finn, E.S. Ghareh Naz et al., Optical microtube cavities monolithically integrated on photonic chips for optofluidic sensing. Opt. Lett. **42**, 486–489 (2017)
25. A. Madani, M. Kleinert, D. Stolarek, L. Zimmermann, L. Ma, O.G. Schmidt, Vertical optical ring resonators fully integrated with nanophotonic waveguides on silicon-on-insulator substrates. Opt. Lett. **40**, 3826–3829 (2015)
26. S. Sedaghat, A. Zarifkar, Tunable optical filter based on self-rolled-up microtube incorporating nematic liquid crystal. Opt. Mater. **67**, 113–118 (2017)
27. S. Sedaghat, A. Zarifkar, Vertical integration of self-rolled-up microtube and silicon waveguides: a two-channel optical add–drop multiplexer. Chin. Opt. Lett. **15**, 022501.1–022501.5 (2017)
28. S. Sedaghat, A. Zarifkar, Evanescent coupling of asymmetric self-rolled-up microtube and slab waveguide. Opt. Commun. **382**, 167–175 (2017)
29. D. Karnaushenko, D.D. Karnaushenko, D. Makarov, S. Baunack, R. Schäfer, O.G. Schmidt, Self-assembled on-chip-integrated giant magneto-impedance sensorics. Adv. Mater. **27**, 6582–6589 (2015)
30. S. Schwaiger, M. Bröll, A. Krohn, A. Stemmann, C. Heyn, Y. Stark et al., Rolled-up three-dimensional metamaterials with a tunable plasma frequency in the visible regime. Phys. Rev. Lett. **102**, 163903.1–163903.4 (2009)
31. A. Madani, S. Böttner, M.R. Jorgensen, O.G. Schmidt, Rolled-up TiO_2 optical microcavities for telecom and visible photonics. Opt. Lett. **39**, 189–192 (2014)
32. S.M. Weiz, M. Medina-Sánchez, O.G. Schmidt, Microsystems for single-cell analysis. Adv. Biosyst. **2**, 1700193 (2018)
33. S. Böttner, S. Li, M.R. Jorgensen, O.G. Schmidt, Vertically aligned rolled-up SiO_2 optical microcavities in add-drop configuration. Appl. Phys. Lett. **102**, 251119.1–251119.4 (2013)
34. R. Songmuang, A. Rastelli, S. Mendach, O.G. Schmidt, SiO_x/Si radial superlattices and microtube optical ring resonators. Appl. Phys. Lett. **90**, 091905.1–091905.3 (2007)
35. X. Yu, E. Arbabi, L.L. Goddard, X. Li, X. Chen, Monolithically integrated self-rolled-up microtube-based vertical coupler for three-dimensional photonic integration. Appl. Phys. Lett. **107**, 031102.1–031102.5 (2015)
36. V.Y. Prinz, V.A. Seleznev, A.K. Gutakovsky, A.V. Chehovskiy, V.V. Preobrazhenskii, M.A. Putyato et al., Free-standing and overgrown InGaAs/GaAs nanotubes, nanohelices and their arrays. Phys. E Low Dimens. Syst. Nanostruct. **6**, 828–831 (2000)
37. S. Böttner, Sh Li, J. Trommer, S. Kiravittaya, O.G. Schmidt, Sharp whispering-gallery modes in rolled-up vertical SiO2 microcavities with quality factors exceeding 5000. Opt. Lett. **37**, 5136–5138 (2012)

Journal : **Large 340** | Article No : **7339** | Pages : **11** | MS Code : **7339** | Dispatch : **7-11-2019**

Journal:	**340**
Article:	**7339**

Author Query Form

Please ensure you fill out your response to the queries raised below and return this form along with your corrections

Dear Author

During the process of typesetting your article, the following queries have arisen. Please check your typeset proof carefully against the queries listed below and mark the necessary changes either directly on the proof/online grid or in the 'Author's response' area provided below

Query	Details Required	Author's Response
AQ1	Kindly check and confirm the inserted city name is correctly identified for affiliation 2.	
AQ2	Kindly check and confirm the corresponding affiliation is correctly identified.	
AQ3	Kindly check and confirm the abstract statement is correctly identified.	
AQ4	Please check the term 'apricated ' in the article and amend if necessary.	
AQ5	Kindly check and confirm the section headings are correctly identified.	
AQ6	Please check the edit to the sentence 'Owing to the asymmetric geometry of RUM…'	
AQ7	Kindly check and confirm the partlables for Figure 2, 4, 5, 6 and 8 is correctly identified.	
AQ8	Please check the edit to the sentence 'As the results from TIRS show, it can be increased from …'	
AQ9	Please check the edit to the sentence 'As a conclusion and prior to the experimental part, the TOC of both …'	
AQ10	Please check the edit to the sentence 'A theoretical study of athermal resonators-based on-chip hybrid RUMs was conducted, followed …'	
AQ11	Please check the edit to the sentence 'However, this drawback of using TiO2 microtubes can be easily addressed …'	